JOURNAL OF CATALYSIS **175,** 226–235 (1998)
ARTICLE NO. CA982017

Transmission Electron Microscopy, Energy Dispersive X-Ray Spectroscopy, and Chemisorption Studies of Pt–Ge/γ-Al_2O_3 Reforming Catalysts

Z. Huang,[1] J. R. Fryer, C. Park, D. Stirling,[2] and G. Webb

Department of Chemistry, University of Glasgow, Glasgow G12 8QQ, United Kingdom

Received August 6, 1997; revised October 27, 1997; accepted December 10, 1997

A series of Pt–Ge/γ-Al_2O_3 reforming catalysts have been prepared and studied by transmission electron microscopy (TEM), energy dispersive X-ray spectroscopy (EDX), and chemisorption. The catalyst performance in the reforming of octane was found to be dependent on the way in which the catalyst had been prepared, selectivity to aromatics being highest when the catalyst had been prepared by a coimpregnation route. The majority of the platinum was in the form of very small particles which could not be seen by the microscope, whereas either all or the majority of the germanium was in the ionic state. PtGe, Pt_3Ge_2, and Pt_3Ge particles were found, together with platinum, in the bimetallic catalysts. Particle aggregation and alloy formation was observed for all the catalysts after they had been used in octane reforming. © 1998 Academic Press

INTRODUCTION

The addition of a second metal (e.g., Re, Sn, Ir, or Ge) to Pt/γ-Al_2O_3 improves both the selectivity to aromatics and the stability of the catalyst in catalytic reforming reactions. Extensive studies have been reported for Pt–Re/γ-Al_2O_3 and Pt–Sn/γ-Al_2O_3 bimetallic catalysts (1–4). There is some contention as to whether rhenium or tin are partially alloyed with the platinum, when used in reforming, and in what oxidation states nonalloyed rhenium or tin are found.

Relatively few papers have been published on Pt–Ge/γ-Al_2O_3 catalysts. There is some controversy as to whether the active germanium species in the reforming catalyst is Ge(II) or Ge(0) and whether it is dispersed or alloyed. Goldwasser *et al.* (5) found that Pt impregnated as H_2PtCl_6 could be fully reduced to Pt(0) after treatment in H_2 at 773 K but the reducibility of Ge(IV) increased with an increase in germanium loading in the precursors to Pt–Ge/γ-Al_2O_3 catalysts with 1% Pt and 0–1% Ge loadings. The catalytic activities for the hydrogenation of benzene and the hydrogenolysis of n-butane were also found to decrease with increasing loading of Ge on the Pt/γ Al_2O_3 and it was suggested that the change in the electronic properties of small platinum particles was responsible for the change in the behaviour of the bimetallic catalysts.

The oxidation state of the active germanium species in Pt–Ge/γ-Al_2O_3 catalysts has also been shown to be dependent on the reduction conditions. Bouwman and Biloen (6) used XPS to determine that it was difficult to reduce Ge(IV) in hydrogen in the absence of platinum, and at 923 K the germanium was soluble in the γ-Al_2O_3 matrix. In the presence of platinum, the catalyst was thought to contain Ge(IV) and Ge(II) species after hydrogen treatment at 823 K, while after reduction at 923 K it contained Ge(II) and Ge(0) species, the latter alloyed with platinum. Miguel *et al.* (7, 8) used TPR and chemisorption methods to show that Pt(IV) could be fully reduced in 5% H_2/N_2 to active free Pt(0) particles by 623 K, whereas the germanium was present as Ge(II) and Ge(IV) in 0.3 wt% Pt/0.3 wt% Ge/γ-Al_2O_3 catalysts, and the primary function of the germanium was to dilute the concentration of Pt(0) particles on the γ-Al_2O_3 support. After reduction at 1123 K, the germanium was found predominantly in the zero-valent state and was thought to be alloyed with platinum. After reduction at 573 K, the dehydrogenation activity of the bimetallic catalyst was comparable to that of Pt/γ Al_2O_3, but its hydrogenolysis activity was about 4.5 times lower than that for the monometallic catalyst. However, after reduction at temperatures greater than 623 K, when some of the Ge(IV) is reduced to Ge(0) and interacts with the Pt(0), the Pt/Ge/γ-Al_2O_3 catalyst was virtually inactive for both hydrogenolysis and dehydrogenation, indicating that alloying may be detrimental in the preparation of active Pt/Ge/γ Al_2O_3 catalysts.

Generally, information regarding the distribution and the chemical state of germanium; the interaction between

[1] Present address: School of Industry and Manufacturing Science, Cranfield University, Cranfield, Bedfordshire MK43 0AL, United Kingdom.

[2] To whom all correspondence should be addressed. E-mail: D.Stirling @chem.gla.ac.uk.

0021-9517/98 $25.00

germanium, platinum, and the support, the tendency of platinum and germanium to form alloys and the role of alloy formation in controlling catalyst performance is required in order to gain an understanding of the bimetallic effects in these reforming catalysts. The term "alloy" used in this context does not necessarily refer to the composition for bulk alloy formation, but rather, it refers to two elements in the metallic state which are in intimate contact with each other. Such metal composites are sometimes referred to as bimetallic clusters and we do not attempt to differentiate the terms alloy and bimetallic cluster in this paper. Here, we report a study of the characterisation of Pt–Ge/γ-Al_2O_3 reforming catalysts using transmission electron microscopy (TEM), micro-beam diffraction (MBD), energy dispersive X-ray spectroscopy (EDX), and chemisorption techniques, and we link the structural properties of these catalysts to their activities and selectivities in n-octane reforming.

METHODS

1. Catalysts

Supported bimetallic Pt/Ge catalysts were prepared with loadings of platinum and germanium of either 0.3 wt% or 1.0 wt% and a constant Pt/Ge weight ratio of unity. Commercial pelletised γ-Al_2O_3 (CK300, BET area 180 m^2) consisting of cylindrical pellets about 2 mm in diameter and ranging from 2 mm to 10 mm in length was used as the support. All the catalysts were prepared by impregnation of the γ-Al_2O_3 support with appropriate concentrations of platinum as H_2PtCl_6 in dilute HCl and/or germanium as a hydrochloric solution of Ge(IV) (germanium ICP/DCP standard solution, Aldrich), followed by a calcination and reduction treatment as detailed below.

a. Pt/Ge catalysts prepared by successive impregnation with germanium and platinum salts. γ-Al_2O_3 pellets were impregnated with the required concentration of Ge(IV) in dilute HCl, dried for 4 h at 383 K in flowing air and then impregnated with the required concentration of H_2PtCl_6 solution before drying again at 383 K in flowing air and calcining and reducing these precursors. Catalysts prepared by this route include catalyst A which contained 0.3 wt% Pt and 0.3 wt% Ge supported on γ-Al_2O_3, and catalyst D which contained 1.0 wt% Pt and 1.0 wt% Ge supported on γ-Al_2O_3.

b. Pt/Ge catalysts prepared by successive impregnation with platinum and germanium salts. The preparation procedures were the same as those described for catalysts A and D above except that the first impregnation was carried out using the H_2PtCl_6 solution and the second using the germanium solution. Catalyst B was prepared by this route and contained 0.3 wt% Pt and 0.3 wt% Ge supported on γ-Al_2O_3.

c. Pt/Ge catalyst prepared by coimpregnation. Pellets of γ-Al_2O_3 were coimpregnated with appropriate amounts of the H_2PtCl_6 solution and the germanium solution in dilute HCl, and then dried in flowing air for 4 h at 383 K, calcined, and reduced as described below. Catalyst C was prepared by this route and contained 0.3 wt% Pt and 0.3 wt% Ge supported on γ-Al_2O_3.

d. Ge catalyst. γ-Al_2O_3 pellets were impregnated with the appropriate amount of germanium solution and then dried in flowing air for 4 h at 383 K, calcined, and reduced. Catalyst E was prepared by this route and contained 0.3 wt% Ge supported on γ-Al_2O_3.

EUROPT-3 (0.3 wt% Pt/γ-Al_2O_3, 0.95 wt% Cl) was used as a reference for comparison.

All the catalyst precursors were subjected to the following calcination and reduction steps:

(i) Calcination. The catalyst precursors were heated from room temperature to 673 K at 5 K min^{-1} in flowing air (60 cm^3 min^{-1}) and held at this temperature for 4 h and then cooled down to room temperature.

(ii) Flushing. He (60 cm^3/minute) was passed over the calcined catalyst precursors for 1 h at ambient temperature.

(iii) Reduction. The reduction was carried out in flowing H_2 (60 cm^3 min^{-1}), with a programmed temperature increase of 5 K min^{-1} from room temperature to 673 K and maintained at this temperature for 2 h. The catalysts were then cooled to room temperature in flowing dihydrogen.

Reoxidation, flushing, and reduction procedures were repeated for the above treated samples to investigate any further changes in the catalysts. Finally, passivation was carried out with 1.0 vol% air/He for samples used for TEM investigations.

2. Catalyst Testing

n-Octane reforming was carried out in a continuous flow microreactor, described elsewhere (9), in which the reaction conditions were as follows: H_2/octane ratio = 6/1; reaction temperature 783 K; reaction pressure 110 psig and weight hourly space velocity (WHSV) 2 hr^{-1}. Analysis of the reaction products was carried out by sampling to a Shimadzu gas chromatograph.

3. Carbon Monoxide and Oxygen Chemisorption

For the chemisorption studies, each catalyst precursor was calcined in flowing air at 673 K for 4 h prior to reduction at 673 K. Chemisorption of either carbon monoxide or dioxygen was performed in the same manner as described in an earlier publication (10).

4. Electron Microscopy and EDX

The microscope used was an ABT-EM002B in which an EDX system LINK2000-QX with a windowless detector

was installed. The microscope was operated at 200 kV. An improved LaB_6 filament was used. The energy resolution of the EDX system was 138 eV at 5.9 keV. TEM specimens were prepared as described previously (10). The procedures used for the microscopy and quantitative EDX analysis have been described (11).

RESULTS

1. Carbon Monoxide and Dioxygen Chemisorption

The chemisorption results are presented as the number of molecules of either carbon monoxide or dioxygen adsorbed per platinum atom in the sample (Table 1). Carbon monoxide is known to adsorb on the platinum surface in both bridged and linear form with the latter predominating (12). The maximum number of CO molecules that can be adsorbed per surface platinum atom was assumed to be 0.75 (10, 13, 14) for calculating the platinum dispersions. We also assumed an O/Pt stoichiometry of unity (10, 12–14).

Metallic platinum adsorbs both dioxygen and carbon monoxide but metallic germanium only adsorbs dioxygen (15). The 0.3 wt% Ge/γ-Al_2O_3 catalyst did not adsorb dioxygen at room temperature after reduction at 673 K. This suggests that the germanium was in an ionic state in the 0.3 wt% Ge/γ-Al_2O_3 catalyst after reduction at 673 K, in agreement with previous investigations (6, 8). The reliability of dioxygen chemisorption measurements for measuring dispersion was confirmed using EUROPT-3. The dispersion obtained for EUROPT-3 from dioxygen chemisorption studies was in close agreement with the EUROPT-3 dispersion measured by carbon monoxide chemisorption.

TABLE 1

CO and O_2 Chemisorption Results for Pt–Ge/γ-Al_2O_3 Catalysts

Catalyst	Adsorbate	Number of molecules per gram catalyst [$*10^{18}$]	Platinum dispersion[a]	Surface (Pt + Ge)[b] total Pt
0.3Pt	CO	5.00	72%	
EUROPT-3	O_2	3.24		70%
A	CO	4.15	60%	
0.3Pt–0.3Ge	O_2	2.64		57%
B	CO	3.31	48%	
0.3Pt–0.3Ge	O_2	1.95		42%
C	CO	2.95	42%	
0.3Pt–0.3Ge	O_2	2.36		51%
D	CO	8.45	37%	
1.0Pt–1.0Ge	O_2	7.10		46%
E	CO	0		
0.3Ge	O_2	0		

[a] Calculated assuming the surface stoichiometry CO : Pt = 0.75 : 1.
[b] Calculated assuming that the surface stoichiometry, O : Pt = 1 : 1 and O : Ge = 1 : 1.

TABLE 2

Microreactor n-Octane Reforming Experiment for Pt–Ge/γ-Al_2O_3 Catalysts

Catalysts	Time on stream/h	% Selectivity to aromatics		% Conversion of octane	
		Initial	Steady	Initial	Steady
EUROPT-3 (0.3Pt)	55	35.2	41.8	48.4	27.3
A (0.3Pt–0.3Ge)	74	18.0	28.9	26.4	29.2
B (0.3Pt–0.3Ge)	76	17.6	39.1	32.0	31.3
C (0.3Pt–0.3Ge)	95	18.1	49.6	33.2	34.3
D (1.0Pt–1.0Ge)	75	29.1	21.0	25.5	15.2
E (0.3Ge)	95	7.8	5.1	7.7	4.8

If metallic germanium was formed in the bimetallic catalysts, one would expect more dioxygen adsorption than in the monometallic catalyst even if the CO adsorption was the same. Additional dioxygen adsorption was observed for catalysts C and D (Table 1) after reduction at 673 K. The excess adsorption of oxygen was used to estimate the amount of metallic germanium in the bimetallic catalysts. Two assumptions were made: (i) The ratios of adsorbed CO and oxygen to platinum ($CO/Pt_{surface} = 0.75$ and $O/Pt_{surface} = 1.0$) were not changed by germanium, (ii) germanium adsorbs oxygen as GeO. The results indicated that only about 3.2 and 3.5% of the germanium was reduced to the metallic state after the reduction in hydrogen at 673 K for catalysts C and D, respectively, the remainder being retained in the ionic state. No additional dioxygen adsorption was found for catalysts A and B after reduction at 673 K, indicating that no germanium was reduced to the metallic state for these two bimetallic catalysts.

2. Octane Reforming

The conversion of n-octane and the selectivity to aromatics for each of the Pt–Ge/γ-Al_2O_3, Ge/γ-Al_2O_3, and EUROPT-3 catalysts are given in Table 2. The activity and selectivity to aromatics for the 0.3 wt% Ge/γ-Al_2O_3 catalyst was very low. Initially, EUROPT-3 had the highest overall conversion and selectivity to aromatics, but its overall activity declined during the catalytic run and had not reached a steady state even after 50 h on stream. The activities and selectivities of the bimetallic catalysts were dependent on both the metal loadings and the way in which the catalysts had been prepared. The steady state activity and selectivity of catalyst D (1.0 wt% Pt–1.0 wt% Ge/γ-Al_2O_3) was lower than the activity and selectivity for each of the 0.3 wt% Pt–0.3 wt% Ge/γ-Al_2O_3 catalysts and EUROPT-3. The highest overall conversion and selectivity to aromatics was obtained using the catalyst prepared by the coimpregnation route (catalyst C). A more detailed analysis of the results will be published separately (9).

In general, the steady state selectivities to hydrogenolysis products of all the Pt–Ge/γ-Al_2O_3 catalysts were about 5%

TABLE 3

Summary of TEM and EDX Results for Pt–Ge/γ-Al_2O_3 and Ge/γ-Al_2O_3 Catalysts

	0.3Pt–0.3Ge A	0.3Pt–0.3Ge B	0.3Pt–0.3Ge C	1.0Pt–1.0Ge D	0.3Ge E
Calcined	x	x	x	x	x
Reduced	x	<20 nm a few Pt particles	<20 nm Pt & Pt-rich Pt–Ge particles	<20 nm Pt–Ge & Pt particles	x
Reoxidised	<5 nm a few Pt particles	<5 nm a few Pt particles	<10 nm Pt particles	<20 nm Pt & Pt–Ge particles	x
Second reduction	<5 nm a few Pt particles	<5 nm a few Pt particles	<10 nm Pt & Pt-rich Pt–Ge particles	<20 nm many Pt & Pt–Ge particles	x
Second reoxidation			<10 nm Pt particles	<20 nm many Pt & Pt–Ge particles	
Third reduction			<10 nm Pt & Pt-rich Pt–Ge particles	<20 nm many small Pt & Pt–Ge particles	
After use in reforming	<30 nm a few Pt and Pt–Ge particles	<30 nm a few Pt & Pt–Ge particles	<40 nm Pt–Ge & Pt particles	<100 nm Pt–Ge & Pt particles	

Note. "x" indicates that no particles were observed in the sample.

and were much lower than those for EUROPT-3 (16%). The steady state selectivities of all the Pt–Ge catalysts for isomerised products were all lower than the steady state isomerisation selectivity for EUROPT-3. The steady state hydrocracking activity was enhanced by the addition of germanium and, in the case of catalysts A, B, and D, increased by a factor of three, compared with the steady-state hydrocracking activity observed for EUROPT-3. Overall, the addition of germanium to Pt/γ-Al_2O_3 increased the overall stability of the catalyst and, in the case of catalyst C, the steady-state selectivity to aromatisation was higher than that of EUROPT-3.

3. *TEM and EDX*

(a) General observations. A brief survey of the TEM and EDX results is summarised in Table 3, where "x" indicates that no particles were observed in the sample. As we have reported for other reforming catalysts (10, 16), the appearance of the alumina crystallites were the same for all the catalysts studied. The alumina crystals were randomly orientated in different directions and showed a range of contrast between the differently orientated crystals.

(b) Catalysts after calcination and reduction, reoxidation, or further reduction/oxidation cycles. A camera length of 11 cm was used for most of the EDX studies. The camera length of the MBD mode was calibrated using a platinum particle observed in catalyst C after calcination, reduction, and reoxidation. The MBDP of this particle was indexed to the [110] zone axis pattern of platinum. A camera length of 71 mm was also used in some experiments and this was calibrated in the same way. Figure 1a shows an image for catalyst C after reoxidation and a third reduction. The EDX results for one of the two particles is shown in Fig. 1b. Both particles were found to be platinum, and the inserted MBDP for one particle was indexed as the [112] zone axis pattern of the platinum. The Al and O came from the γ-Al_2O_3 support, C from the carbon film, and Cu from the copper grid and the specimen holder.

Generally speaking, there were only a few particles in catalyst A, and all of the particles were platinum. A similar trend was observed for catalyst B before it was used in n-octane reforming reactions. This suggests that most of the platinum and germanium in the catalysts was not present as large particles (>1 nm), as they would be visible under the microscope even though they were deposited on an alumina support. A similar conclusion was drawn from TEM and EDX studies of Pt–Re/γ-Al_2O_3 and Pt–Sn/γ-Al_2O_3 catalysts (10, 16). Furthermore, analysis of a 0.5 wt% Pt/γ-Al_2O_3 catalyst by X-ray diffraction, high resolution electron microscopy, and dihydrogen chemisorption (17) showed that the average platinum particle size was 0.9 nm, in accordance with our observations.

Pt–Ge alloy particles were observed at metal loadings of 1.0 wt% (catalyst D). Many small particles (about 1–2 nm in diameter) were observed for this catalyst after reoxidation and a third reduction step. Most of these small particles were platinum, but some particles were found to be Pt-rich

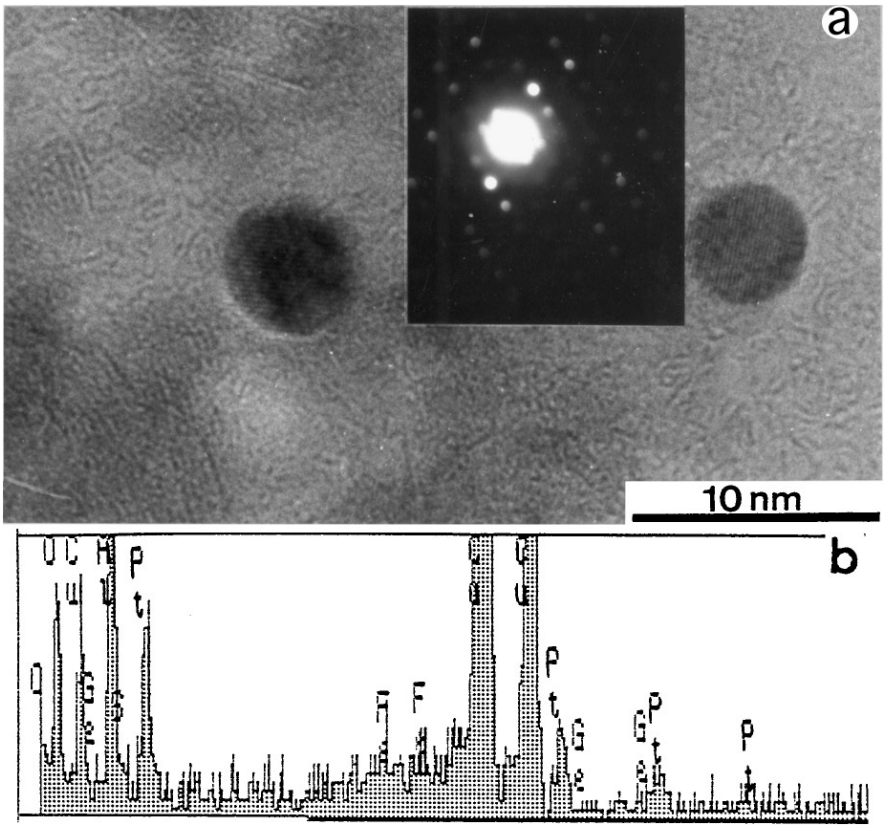

FIG. 1. Catalyst C after reoxidation and a third reduction: (a) TEM micrograph and inserted MBDP; (b) EDX spectrum from one of the particles.

Pt–Ge bimetallics. The Pt–Ge particles may in fact have been present as solid solutions since the Pt/Ge elemental ratio for the particles varied from 10 to 20. Twin platinum particles were also observed in this catalyst (Fig. 2). The corresponding MBDP (the insert) shows that the particle was a [110] twin of platinum.

No particles were observed in the 0.3 wt% Ge/γ-Al_2O_3 catalyst after calcination and reduction.

(c) Catalysts after use in octane reforming. Most of the larger particles (>4 nm in diameter) in the catalysts were found to be alloy particles after the catalysts had been used in octane reforming. Most of the smaller (<4 nm) particles and a minority of the larger particles were platinum. Figure 3A(a) shows the image of a particle for the catalyst C after use in octane reforming. The particle consisted of three different regions X, Y, and Z as marked on the picture. The EDX results presented in Fig. 3A(b) showed that the elemental ratio for the whole particle was Pt/Ge = 2.02. EDX results also indicated that region X was platinum and the atomic ratios for regions Y and Z were Pt/Ge = 2.57 and 1.65, respectively. The MBDP (insert X) for X was the [110] pattern for platinum. The MBDP (insert Z) for region Z could not be indexed because it was not a zone axis pattern. Other particles indexed to the [102] zone axis pattern of the orthorhombic PtGe and Pt_3Ge_2 structures were also observed in this catalyst. Figure 3B(a) shows the image of a particle with its MBDP being indexed to the [031] pattern of the Pt_3Ge_2 and the EDX results in Fig. 3B(b) showed that the elemental Pt/Ge ratio for the particle was 1.74. Double diffraction was observed in this crystal and some diffraction spots (indicated on the MBDP insert) disappeared when the crystal was slightly tilted. Some other particles were observed to have the same [031] MBDP corresponding to the Pt_3Ge_2 structure but with a Pt/Ge ratio of 1.34. It is possible that the differences in EDX patterns for particles with the same MBDP may simply have been due to a second phase such as platinum present in one of the particles as was the case for the particle shown in Fig. 3A. However, the EDX spectrum and MBDP for each particle were not necessarily taken at the same crystal orientation. This has been shown to affect the observed EDX spectrum (18, 19) and may offer an alternative explanation for the differences in EDX results. Systematic errors present in the EDX setup may also have contributed to the variance in results and one should be cautious about drawing conclusions about particle structure based solely on EDX results. However, it can provide complementary information when combined with microbeam electron diffraction studies. Microbeam electron diffraction has proved to be a powerful

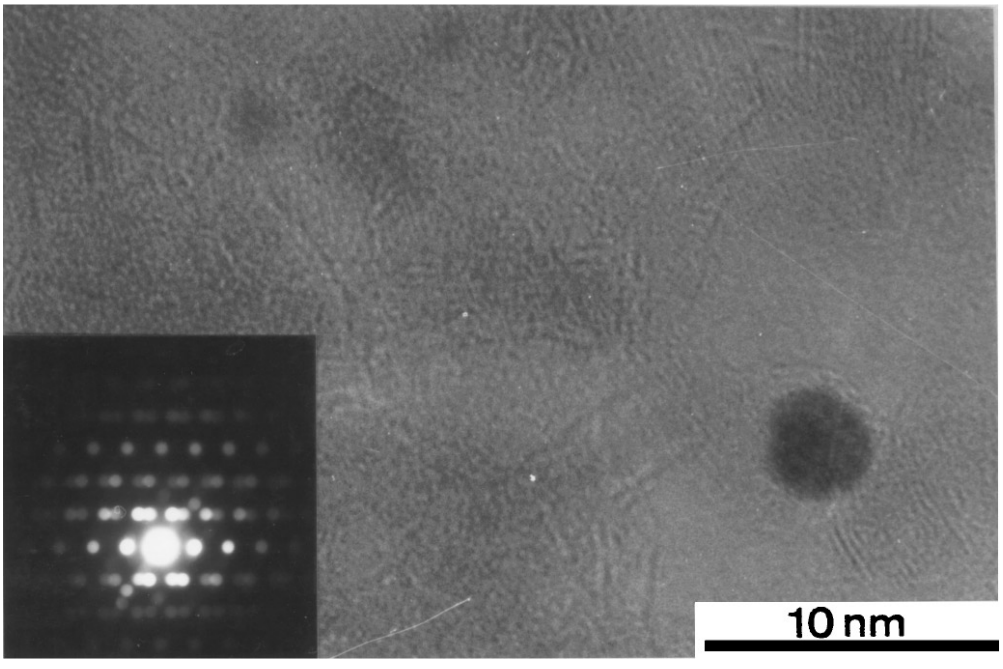

FIG. 2. Catalyst D after reoxidation and a third reduction. TEM micrograph of twin platinum crystal and MBDP insert.

technique for determining the structure of small particles (20, 21).

Figure 3C(a) shows the image of a particle for catalyst C after being used in octane reforming. EDX results indicated that this particle was mainly platinum. However, the MBDP shown in Fig. 3C(b) taken from the section of the particle indicated by arrows on the micrograph did not match any of the diffraction patterns for known Pt–Ge(11). The EDX spectrum from this part of the particle indicated the presence of germanium. It was noted that the bright (strong) spots of the MBDP matched exactly the [110] pattern of the face-centred-cubic (FCC) platinum structure. There was also an extra diffraction spot between each pair of bright (strong) diffraction spots. The whole MBDP could therefore be indexed as the [110] pattern of a FCC structure with a lattice dimension double the size of platinum lattice dimension a_{Pt}. We therefore concluded that this particle had a superlattice structure with the lattice dimension $a = 2a_{Pt}$. Further work later showed that this phase has the formula Pt_3Ge(11). Most of the particles detected in catalysts A and B after they had been used in n-octane reforming were Pt–Ge alloys.

There was a substantial increase in the number of particles in the 1.0 wt% Pt–Ge/γAl_2O_3 catalyst (catalyst D) after it had been used in octane reforming reactions. The majority of the particles were Pt–Ge alloys and the minority were platinum. Figure 4 shows an image for catalyst D after use in octane reforming. It clearly showed that one particle was deposited on another larger particle. The EDX spectrum indicated that the smaller particle was platinum and the MBDP (inserted) for the particle was the [110] pattern for platinum. Moreover, some weak additional diffraction spots were found in the diffraction pattern, as for the case in Fig. 3C(b). It is likely that these extra spots originated from the diffraction of the larger particle lying under the smaller platinum particle. The larger particle had lattice fringe spacings double the size of the lattice fringes of the smaller particle, as marked on the picture, which indicated that the particle had the superlattice structure Pt_3Ge previously reported (Fig. 3C).

It should be emphasised that even after reforming, the areas on the TEM images with visible metal particles accounted for only a very small part of the total area investigated. However, even in those areas where no particles were visible, EDX studies clearly showed the presence of both platinum and germanium. This suggests that platinum and germanium existed as either very small particles (<1 nm) or particles closely associated with the alumina support even after the catalysts had been used in reforming.

DISCUSSION

The chemisorption studies for all the Pt–Ge (0.3–0.3 wt%)/γ-Al_2O_3 catalysts showed that, whereas platinum (IV) was fully reduced to platinum (0) partial reduction (3.2%) of the Ge(IV) was only observed in catalyst C after treatment in dihydrogen at 673 K. This demonstrates that the reducibility of the germanium species depends on the way in which the catalyst has been prepared. These results can be contrasted with studies carried out by Miguel *et al.* (7), who prepared Pt–Ge (0.3–0.3 wt%)/Al_2O_3 catalysts by coimpregnation and successive impregnation

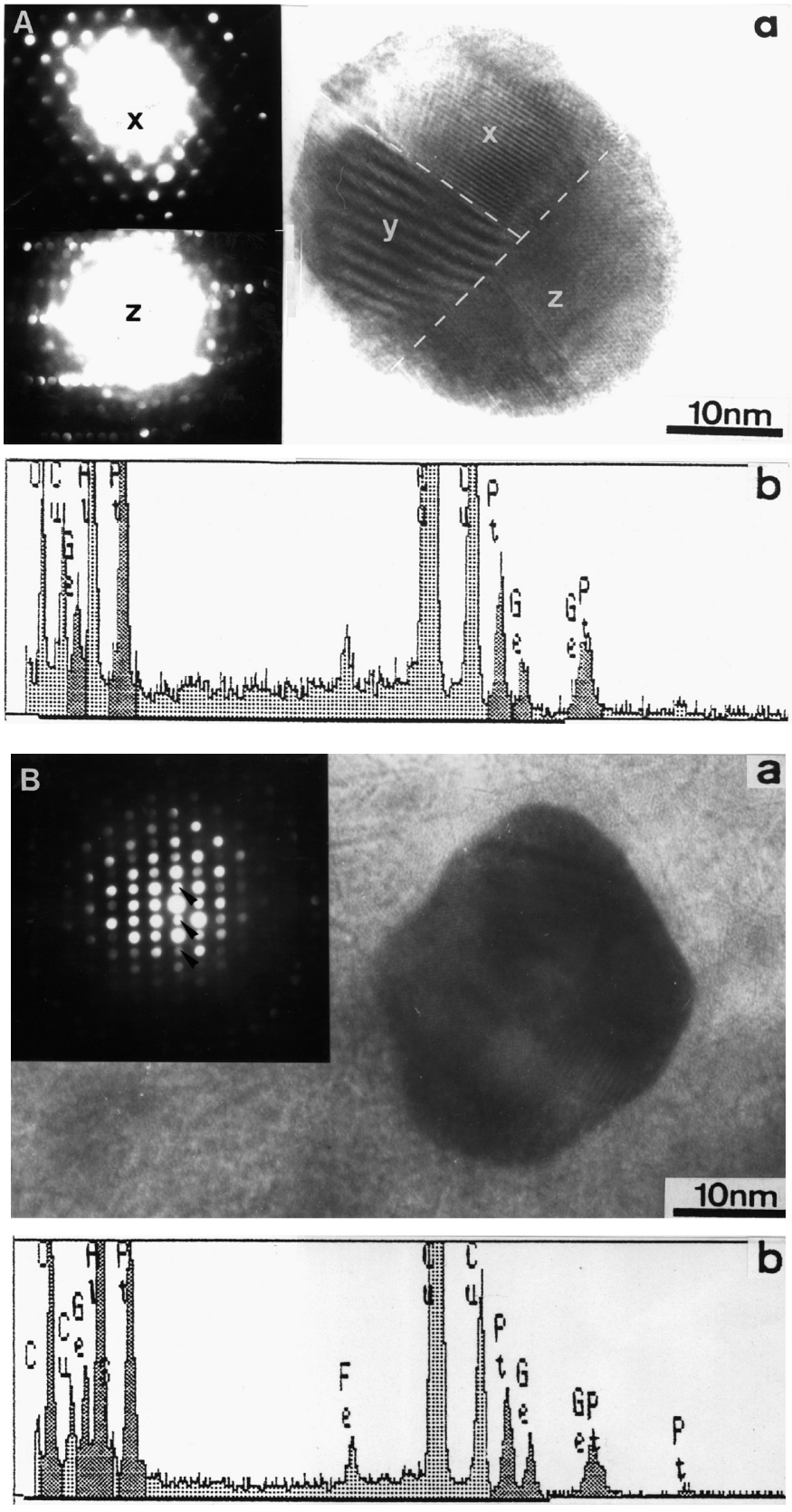

FIG. 3. Catalyst C after use in octane reforming. A. (a) TEM micrograph of particle consisting of three different regions X, Y, and Z, and corresponding MBDP for regions X and Z (insert); (b) EDX spectrum for the whole particle. B. (a) TEM micrograph and inserted MBDP corresponding to Pt_3Ge_2; (b) EDX spectrum shows the elemental ratio was Pt/Ge = 1.74 for the particle. C. (a) TEM micrograph, (b) MBDP corresponding to a superlattice structure.

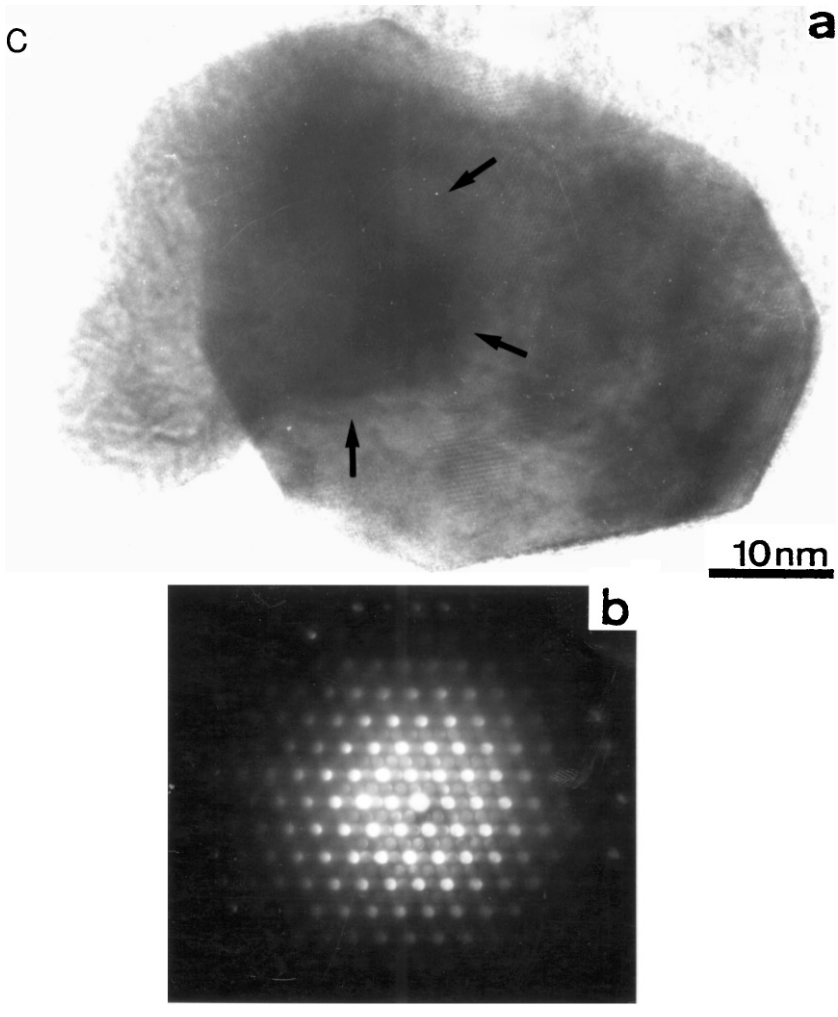

Fig. 3—*Continued*

methods and found that the TPR reduction profiles for each of these catalysts was similar, with reduction of the platinum species occurring at 548 K and the germanium species at around 873 K.

Our results showed that on increasing the platinum and germanium loadings from 0.3 wt% to 1.0 wt% (catalyst D) platinum (IV) was again fully reduced to Pt(0) and very little of the germanium (IV) was reduced after the calcined precursor had been treated in dihydrogen at 673 K in accordance with previous observations (5). Similar effects have been reported by Burch (22) in studies of the oxidation state of tin in the related Pt–Sn/Al_2O_3 catalyst. He found that the average oxidation state of the tin after reduction of Pt(IV)–Sn(IV)/Al_2O_3 was Sn(II) and that this was independent of the tin loading over the concentration range 0.3–5.0 wt%. In our calculations we assumed that the platinum dispersion was not affected by the germanium. However, it is possible that this was not the case, so that the dispersions observed for catalysts C and D may have been due to increased platinum dispersion with the germanium either remaining as Ge(IV) or being reduced to Ge(II). The TEM results do not support this hypothesis, however, as platinum particles were observed in catalysts C and D after reduction indicating that the platinum dispersion was poorer in these catalysts than in EUROPT-3 in which the platinum has been shown to be highly dispersed with no particles detectable by TEM (10).

A high platinum dispersion was retained in catalyst A which was prepared by successive impregnation with Ge(IV) and then Pt(IV), but successive impregnation with Pt(IV) followed by Ge(IV) (catalyst B) or coimpregnation with these salts (catalysts C and D) resulted in a considerable loss in dispersion when compared to EUROPT-3. This indicates that the Ge(IV) may interact with the alumina and stabilise the platinum dispersion more effectively when the catalyst is prepared by impregnating the support with Ge(IV) prior to the Pt(IV) salt. Goldwasser *et al.* (5)

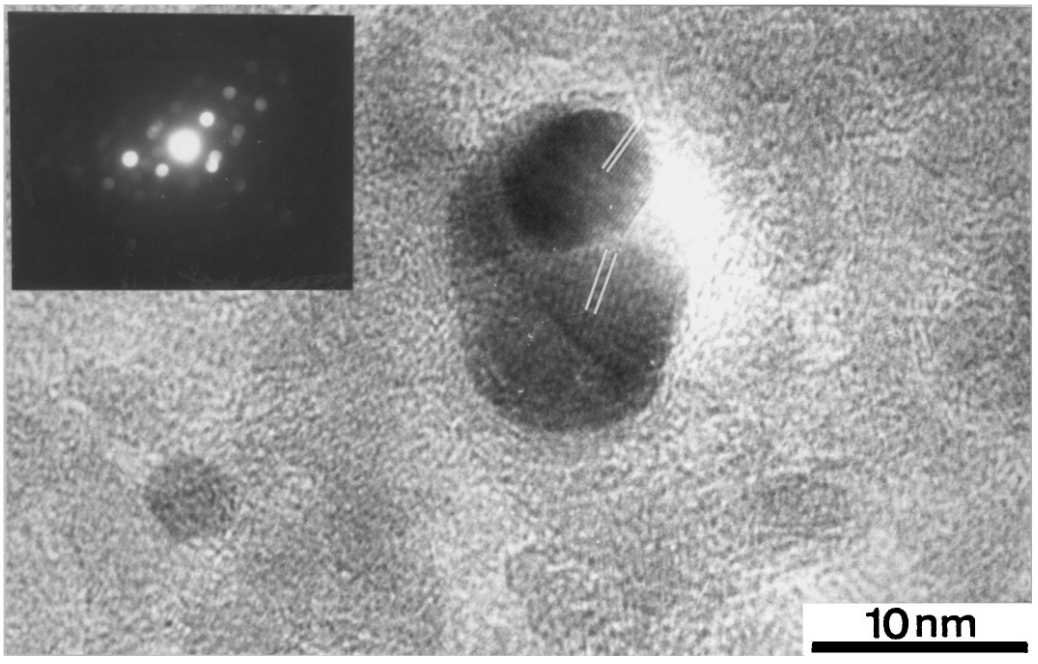

FIG. 4. TEM micrograph of catalyst D after being used in octane reforming. EDX results indicated that the small particle on the large particle was platinum. The strong spots of the inserted MBDP was indexed the [110] pattern of the platinum. The weak diffraction spots suggest the larger particle may have the superlattice structure mentioned in the text.

also observed only a small loss in platinum dispersion on preparing Pt–Ge/Al_2O_3 catalysts by successive impregnation with Ge(IV) and then Pt(IV) compared with Pt /Al_2O_3. Our electron microscopy studies also showed that catalyst A was the only one of the prepared Pt–Ge/γ-Al_2O_3 catalysts which contained no observable particles after its initial preparation by calcination and reduction of the precursor. However, TEM studies showed that, on reoxidation and a second reduction and after use in reforming, catalyst A contained particles of similar composition and particle size to those found in catalyst B.

The observed structural properties of the catalysts can be correlated to their catalytic behaviour. The dispersion observed for catalyst C was poorer than that for the two other Pt–Ge (0.3–0.3 wt%)/γ-Al_2O_3 catalysts. Catalyst C, unlike A and B, also contained Pt-rich Pt–Ge alloy particles, before use in reforming, and yielded the highest steady-state selectivity to aromatics and conversion in n-octane reforming, retaining this activity and selectivity after 95 h on-line. The formation of a few small Pt–Ge alloy particles in catalyst C prior to its use in octane reforming may have diluted the platinum surface in catalyst C by an ensemble effect (23), resulting in its high selectivity to aromatics. The ensemble theory (24) assumes that dehydrogenation reactions can proceed at a single platinum atom, whereas hydrogenolysis requires a row of at least two or three platinum atoms (23). A germanium-diluted platinum surface would therefore be expected to give lower yields of hydrogenolysis products than EUROPT-3 and this was indeed found to be the case. Although no alloy particles were detected in catalysts A and B prior to their use for reforming, most of the particles observed after the catalysts had been used were alloy particles, indicating that dilution of the platinum ensembles occurred during reaction. However, it is clear that some alloy formation prior to use in reforming is beneficial for these Pt–Ge (0.3–0.3 wt%)/γ-Al_2O_3 catalysts, since the steady state selectivity to aromatics was greater than that observed with EUROPT-3 using catalyst C, but less than EUROPT-3 using catalysts A and B. Alloy formation may also lead to some redispersion during the reactivation process, since catalyst C contained platinum-rich Pt–Ge particles after reduction, but smaller platinum particles were formed on reoxidation.

The platinum dispersion and amount of reduced germanium (IV) were similar for catalysts C and D, but a much greater number of Pt–Ge alloy particles, together with some platinum particles, were visible in the 1.0 wt% Pt–1.0 wt% Ge/γ-Al_2O_3 catalyst (catalyst D) after reduction, and the steady-state conversion of octane and selectivity of this catalyst for aromatics was lower than for any of the 0.3 wt% Pt–0.3 wt% Ge/γ-Al_2O_3 catalysts or EUROPT-3. Clearly, concentrations of germanium in excess of 0.3 wt% poison the catalytically active platinum sites. A similar effect was noted by Goldwasser *et al.* (5), who reported that the activity for the hydrogenation of benzene using a Pt–Ge (1.0–0.3 wt%)/γ-Al_2O_3 catalyst was comparable to that of 1.0 wt% Pt/γ-Al_2O_3 and declined rapidly at higher concentrations of germanium.

Although some particles were observed in catalysts B, C, and D on reduction and all the catalysts contained particles after use in reforming, most of which were alloy particles, it should be emphasised that the areas investigated by TEM with visible metal particles on them accounted for only a very small part of the total area investigated. EDX studies revealed the presence of both platinum and germanium in regions of the catalysts where no particles were detected. This indicated that the platinum and germanium either existed as small TEM-invisible (<1 nm) particles, or that they were closely bonded to alumina. Since the Ge(IV) is difficult to reduce (25), it is likely that the germanium would be closely associated with the alumina, although the possible formation of small Pt–Ge alloy particles cannot be discounted on the basis of the evidence available. Pt(IV) is readily reduced to Pt(0), so it is most likely that the platinum will be present in the form of very small TEM-invisible (<1 nm) platinum particles. These platinum particles may be modified by interaction with either germanium or germanium oxide leading to changes in the electronic properties of the platinum, as previously reported for Pt–Sn/Al_2O_3 catalysts (22). It is likely that these electronically modified platinum particles would contribute to the improved stability of the bimetallic reforming catalysts.

The amount of carbon deposited on each of the Pt–Ge catalysts was found to be less than the amount formed on Pt/Al_2O_3 in accordance with previous observations (4). Large platinum ensembles are required for the formation of a carbonaceous overlayer (26), so the dilution of the platinum ensembles by adding germanium to platinum would decrease the coke formation on the metal sites and increase the lifetime of the catalyst.

The hydrocracking activity of all the Pt–Ge catalysts was much higher than that observed for EUROPT-3. This can be explained by the fact that most of the germanium was present as GeO_2 which is very acidic (27) and would thus enhance hydrocracking reactions which are known to occur on acidic sites.

Overall, this study demonstrates that higher selectivities to aromatics can be obtained using Pt–Ge/γ-Al_2O_3 rather than Pt/γ-Al_2O_3 catalysts when the former are prepared by a coimpregnation route. The main function of the germanium is: (i) to dilute the platinum ensembles on the surface of the alumina and, hence, to favour reactions which proceed on single platinum atom sites or small platinum ensembles; and (ii) to increase the stability of the catalyst by modifying both the type and amount of coke that is laid down on the surface.The selectivity to aromatics is critically dependent on the way in which the Pt–Ge/Al_2O_3 catalyst is prepared, and results from a complex interplay between the electronically modified small (<1 nm) platinum particles by germanium or germanium oxide and the formation of Pt–Ge alloys.

ACKNOWLEDGMENTS

Financial support from the Initiative in Interfaces and Catalysis of SERC is gratefully acknowledged. Z Huang thanks Mr. D. Thom for technical help.

REFERENCES

1. Sinfelt, J. H., "Bimetallic Catalysts: Discoveries, Concepts, and Applications." Wiley, New York, 1983.
2. Kluksdahl, H. E., U.S. Patent 3,415,737 (1968).
3. Burch, R., and Garla, L. C., *J. Catal.* **71**, 360 (1981).
4. Beltramini, J., and Trimm, D. L., *Appl. Catal.* **32**, 71 (1987).
5. Goldwasser, J., Arenas, B., Bolivar C., Castro, G., Rodriguez, A., Fleitas, A., and Giron, J., *J. Catal.* **100**, 75 (1986).
6. Bouwman, W., and Biloen, P., *J. Catal.* **48**, 209 (1977).
7. Miguel, S. R. D., Scelza, O. A., and Castro, A. A., *Appl. Catal.* **44**, 23 (1988).
8. Miguel, S. R. D., Correa, J. A. M., Baronetti, G. T., Castro, A. A., and Scelza, O. A., *Appl. Catal.* **60**, 47 (1990).
9. Park, C., and Webb, G., to be published.
10. Huang, Z., Fryer, J. R., Park, C., Stirling, D., and Webb, G., *J. Catal.* **148**, 478 (1994).
11. Huang, Z., Fryer, J. R., Stirling, D., and Webb, G., *Phil. Mag. A* **72**(6), 1495 (1995).
12. Jackson, S. D., Glanville, B. M., Willis, J., McLellan, G. D., Webb, G., Moyes, R. B., Simpson, S., Wells, P. B., and Whyman, R., *J. Catal.* **139**, 207 (1993).
13. Gruber, H. L., *J. Phys. Chem.* **66**, 48 (1962).
14. Benson, J. E., and Boudart, M., *J. Catal.* **4**, 704 (1965).
15. Bond, G. C., "Catalysis by Metals." Academic Press, London, 1962.
16. Huang, Z., Fryer, J. R., Park, C., Stirling, D., and Webb, G., *J. Catal.* **159**, 340 (1996).
17. Butterly, L. J., Baird, T., Fryer, J. R., Day, M., and Norval, S., *in* "Proc. XIth Int. Cong. on Electron Microscopy" (T. Imura, S. Maruse, and T. Suzuki, Eds.), Vol. II, p. 1775. The Japanese Society of Electron Microscopy, Tokyo, 1986.
18. Tafto, J., and Gjonnes, J., *Ultramicroscopy* **26**, 97 (1988).
19. Spence, J. C. H., Kuwabara, M., and Kim, Y., *Ultramicroscopy* **26**, 103 (1988).
20. Morniroli, J. P., and Steeds, J. W., *Ultramicroscopy* **45**, 219 (1992).
21. Redjaimia, A., and Morniroli, J. P., *Ultramicroscopy* **53**, 305 (1994).
22. Burch, R., *J. Catal.* **71**, 348 (1981).
23. Biloen, P., Dautzenberg, F. M., and Sachtler, W. M. H., *J. Catal.* **50**, 77 (1977).
24. Sachtler, W. M. H., *Cat. Rev. Sci. Eng.* **14**, 193 (1976).
25. Bouwman, R., and Biloen, P., *J. Catal.* **48**, 209 (1977).
26. Barbier, J., Corro, G., Zhang, Y., Bournonville, J. P., and Franck, J. P., *Appl. Catal.* **16**, 169 (1985).
27. Krylov, O. V., "Catalysis by Non-Metals." Academic Press, New York, 1973.